ELSEVIER

Thermochimica Acta 323 (1998) 145–157

thermochimica acta

A thermal study of Zr-pillared montmorillonite

M.R. Sun Kou[1], S. Mendioroz*, M.I. Guijarro

Instituto de Catálisis y Petroleoquímica, C.S.I.C., Campus U.A.M., 28049 Madrid Cantoblanco, Spain

Received 6 February 1997; received in revised form 31 July 1997; accepted 11 August 1998

Abstract

Zirconium-pillared montmorillonites have been prepared by different methods in order to investigate their effect on the physico-chemical properties of the resulting interlayered materials. It has been verified that variations in the synthesis procedure, such as concentration of the Zr solution, pH, temperature, and time of contact with the clay, affect the structure and properties of the pillared clays obtained.

The thermal stability and degradation of the samples have been investigated by XRD, TA, FTIR and nitrogen adsorption–desorption isotherms. The dehydroxylation of Zr-pillared clays starts at around 523 K and ends above 1038 K. Over this whole range of temperature, the shape of the thermal curves is different. The differences have been related to the Zr content, the degree of polymerization of the Zr cations, resulting from their aging conditions, and the partial solution of the parent clay by the effect of pH of the pillaring zirconyl chloride solutions.

Keywords: Montmorillonite; Pillared clays; Thermal analysis; Zr-montmorillonite; Zr-PILC

1. Introduction

Pillared interlayered clays (PILCs) comprise a new family of clays, based on two-dimensional materials with a certain porous texture and a structure capable of being used, among others, in adsorption and catalysis. Their preparation usually involves ion exchange of the cations in the interlayer region of the clay by inorganic polyoxycations. These polyoxycations are converted by heat to the corresponding oxides which act as props between the silicate layers, thus generating a microporous material with potential interest as molecular sieve [1,2].

Among the cations used for pillaring, one of the most profusely used up to the present is a polynuclear hydroxy zirconium complex whose structure is $[Zr_4(OH)_{14}\cdot(H_2O)_{10}]^{2+}$ [3–5]. This structure, characterized by X-ray scattering studies [6], is composed of four zirconium units lying at the corners of a square and linked along each edge of the square by a pair of OH groups, located one above, and the other below, the plane of the zirconium ions. In addition, each Zr ion is linked to four additional water and/or hydroxyl groups. But this Zr_4 cation can undergo polymerization, slowly at ambient temperature and quite rapidly at higher temperatures, resulting in different structures and sizes of the cation affecting the interlayer distances and the stability of the resulting materials.

Lopez et al. [7] reported that the crystalline phase and the interactions of the Zr_4 ion with other materials

*Corresponding author. Tel.: +34-1-585-4785; fax: +34-1-585-4760; e-mail: smendioroz@icp.csic.es

[1]On leave from I.C.P. Present address: Universidad Nacional de Ingeniería. Perú. Lima. E-mail:msun@pucp.edu.pe

0040-6031/98/$ – see front matter
PII: S0040-6031(98)00540-1

as SiO_2 depend on the initial synthesis conditions, temperature or time of ageing and pH of the Zr solution, which are necessary to control in order to obtain the desired degree of polymerization of the Zr_4 cation. Also, the effect of the Zr_4 preparation method on the d_{001} spacing, surface area and thermal stability of the resulting Zr-pillared materials has been reported [8,9]; however, the information is scarce and a deeper insight into the causes giving rise to those effects seems profitable. To be useful in catalysis, the pillared clays must have, besides the proper texture so as to facilitate the fast diffusion of reagents within their interlayer space, a good thermal and hydrothermal resistance. In a pillared clay, dehydration and dehydroxylation may depend on

(a) the structure and composition of the parent clay unit cell,
(b) the number and nature of the interchangeable cations [10],
(c) the nature and structure of the incorporated hydroxycation to be converted in oxide props, and
(d) the interaction between the guest and the clay surfaces.

Thereafter, once the oligocation is included, the frame stability, which is controlled by the stability of the intercalated ion and by the strength and nature of the interactions between the guest and the host species, is of fundamental interest. Therefore, knowledge of the changes undergone by a sample on heating, can be of particular interest to derive additional information on the nature and properties of the material.

Farmer and Russell [11,12] have shown that dehydration of the interlayer cations, whether or not they have penetrated the octahedral positions, results in the perturbation in the 600–950 cm^{-1} infrared region. Thus, a knowledge of the changes in the 'OH deformation' region of the infrared spectra of the pillared clays as a result of change in temperature can be of great help in obtaining a good understanding of the position of the interlamellar cations.

The aim of this research is to study, by the TGA and DTA techniques, the dehydration and dehydroxylation behaviour of some Zr-pillared clays synthesized by reacting the montmorillonite with various Zr polymers prepared by different procedures, and to verify the conclusions arrived at by FTIR spectroscopy.

2. Experimental

2.1. Materials

The starting mineral was a bentonite from La Serrata of Nijar, southeast Spain, rich in montmorillonite, supplied by Minas of Gador S.A. The montmorillonite fraction had a cation exchange capacity (CEC) of 61.6 meq per 100 g of clay, a surface area of 87 $m^2\ g^{-1}$ and a pore volume of 0.121 $cm^3\ g^{-1}$. Its structural formula, calculated by the Ross and Hendricks method [13] is:

$$(Si^{4+}_{7.74}Al^{3+}_{0.26})_T(Al^{3+}_{2.5}Fe^{3+}_{0.25}Mg^{2+}_{1.30}Ni^{2+}_{0.003})_O \times O_{20}(OH)_4(Ca^{2+}_{0.21}Na^{+}_{0.85}K^{+}_{0.11})_{CC}$$

In order to prepare the pillared materials, the montmorillonite was purified by conventional sedimentation, the <2 mm fraction collected and, subsequently, exchanged with a 1 M solution of NaCl to obtain Na-montmorillonite (Na-Mont). The homoionic material had a S_{BET}=77 $m^2\ g^{-1}$, V_p= 0.093 $cm^3\ g^{-1}$, d_{001}=12.01 Å. $ZrOCl_2{\cdot}8H_2O$ from Aldrich was used to prepare the pillaring polycations. Zr-pillared montmorillonites were prepared by the following two methods:

1. Adopted from Yamanaka and Brindley [3] with slight modifications: appropriate volumes of $ZrOCl_2{\cdot}8H_2O$ (0.1 M) were added to 5 g of Na-Mont and continuously stirred for 24 h at room temperature.
2. Borrowed from Bartley and Burch [5]: 5 g of Na-Mont were added to the proper volumes of $ZrOCl_2{\cdot}8H_2O$ (0.1 M) previously refluxed for 24 h, and the suspension stirred for 24 h at room temperature.

Afterwards, the clay suspensions were dialyzed against distilled water (1 l/g of clay) until free of chlorides. Finally, the samples were freeze-dried and calcined at 623 and 773 K for 2 h.

The samples will be referred from now on using the code P/*x*/*y*, where *x* is the meq Zr/g clay ratio and *y* indicates the method of preparation of the Zr polymer: stirred (SR) or refluxed (R).

3. Methods

Zr was analyzed by inductively coupled-plasma (ICP) emission spectrometry in a Perkin–Elmer Plasma 40 equipment, using Ar as plasmogene. The surface areas and porosity were determined by nitrogen adsorption at 77 K, using a Micromeritics ASAP 2000 sorptometer: prior to the experimentation, the samples were outgassed at 473 K for 16 h. In surface-area calculation, 0.162 nm^2 for the cross-sectional area of the adsorbed N_2 molecule was used. To evaluate microporosity, the Dubinin–Raduskevicht (DR) plot [14] was used. Basal spacing was evaluated through XRD by using a Siemens diffractometer model Kristalloflex D-500 and CuK_a radiation. The spectra were acquired at 2°/min in the $2<2\theta<75°$ interval.

Thermal analysis was conducted in a Perkin–Elmer TGS-2 with Data Station 3600 and temperature controller system 7/4 for TGA and in a Stanton–Redcroft STA-780 coupled to a DC amplifier and temperature controller DTA 781 and UTP for DTA. Sample weights around 40 mg in the former and 9.5 mg in the latter were used. The systems sensitivity is not <0.2 mg. The analyses were effected in all cases at a heating rate of 20 K/min between 293 and 1273 K and under static air atmosphere. Data from DTA were registered at the rate of 2 mm/min and with a lecture at full scale of 50 mV.

Surface groups were identified in an FTIR equipment Nicolet 5Z-DX model in the 400–4000 cm^{-1} spectral range with a resolution of 2–4 cm^{-1}. A DTGS detector with KBr window and an interferometer, moving at a rate of 0.32 cm/s, complete the set. Samples were prepared with 98% KBr and conformed under 5 kg/cm^2 pressure.

4. Results and discussion

Table 1 shows the pH of the Zr starting solution, and the Zr content, basal spacing, surface area and microporosity of the resulting materials at room temperature (RT), and after a 2-h treatment at 623 and 773 K, respectively.

From Table 1 it appears that the zirconium content in the samples increases with the Zr/clay ratio. However, assuming that all the incorporated zirconium is present as $[Zr_4(OH)_{14}(H_2O)_{10}]^{2+}$ and having in mind the CEC of the parent clay, it appears that the interchange has been completed only in 20SR and 20R samples.

Fig. 1(a) and (b) depict the diffractograms corresponding to the SR and R series, respectively, at ambient temperature and after a 2 h treatment at 623 K. From the figure it is apparent that the line d_{001} can hardly be detected in the samples P20, although the other lines remain detectable. The effect probably should be related to a high disorder of the clay structure resulting from the synthesizing step. In the remaining samples, an increase in the basal spacing of around 7 Å over dry clay is apparent.

In Fig. 2(a) and (b), the isotherms corresponding to the SR and R series are included. All samples experience a significant increase in surface area, micro- and mesoporosity and N_2 uptake with the Zr content more important, in the samples prepared from refluxed Zr. Microporosity, evaluated from the DR plot applied to

Table 1
Starting pH, Zr content, d_{001}, surface area and microporosity of the Zr-PILCs

Sample	pH	Zr%	d_{001}/(nm)		S_{BET}/(m^2/g)			Microporosity/(mm^3/g)		
			298 K	623 K	298 K	623 K	773 K	298 K	623 K	773 K
Na-Mont			1.2		77			33		
P2SR	3.20	4.69	1.5	1.3	126	111	78	53	46	32
P5SR	2.75	6.96	1.7	1.4	183	174	140	76	73	57
P20SR	2.10	9.63	—	—	257	198	149	115	80	63
P2R	2.80	4.50	1.6	1.2	196	162	158	82	68	66
P5R	2.30	6.95	1.6	1.2	264	215	191	111	94	80
P20R	1.96	9.58	—	—	278	243	221	111	100	93

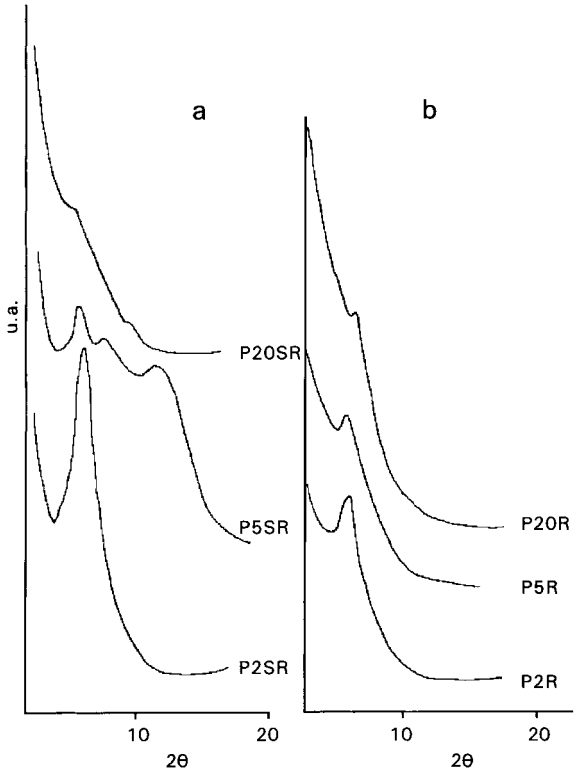

Fig. 1. XRD of pillared samples at 298 K and after 2 h treatment at 623 K: (a) SR series; and (b) R series.

the first terms of the isotherm (p/p_0<0.1), takes the values shown in Table 1. This apparent lack of consistency between the results coming from the two techniques, XRD and N_2 adsorption, should be explained by the occurrence in the samples of a strong delamination as a consequence of the pH of the pillaring starting solution. That delamination, following Occelli [15], is characterized by a house-of-card-like structure which increases the mesoporosity, such as detected through the increase in the isotherms slope, accompanied by a certain microporosity in an FF (face-to-face) short-range association coming from pillaring, which gives rise to the disordered structure shown by XRD in Fig. 1. It is well known that the treatment of clay slurries with mineral acids improve their sorptive and catalytic properties. In a previous work [16], one of the authors showed the effect of increasing concentrations of HCl on a montmorillonite from La Serrata. There, a gradual change from clay delamination to octahedral layer solution occurred, eventually leading to the formation of amorphous silica, accompanied with the corresponding changes in surface area and basal spacing. The same was detected on clays, pillared or not, by Carrado et al. [17]. Thus, at low pH, resulting from the high Zr–clay ratios and the severe ageing conditions of the cationic precursor used, a deeper modification of the clay is likely to occur with delamination and further dissolution of the octahedral layer.

It must be emphasized here that samples P2R and P5SR, becoming from solutions with similar pH, offer quite similar N_2 isotherms and, hence, surface areas and porosities, thereby indicating the influence of the pillaring solution pH in the final characteristics of the materials.

All the samples undergo through calcination at 773 K, a decrease in surface area and microporosity on account of dehydroxylation and final degradation of the Me-oligocations; however, these losses are not as high as expected, especially on series R, thus denoting the stability of the incorporated cations.

4.1. Thermogravimetric analysis

In Fig. 3(a–c) are depicted the thermal curves in the 298–1273 K range, corresponding to the starting Na-Mont and Zr-pillared clays after equilibration in a desiccator, at room temperature and after a 2 h thermal treatment at 623 and 773 K, respectively. The general feature of the thermal curves clearly reveals two steps: one, in the 298–353 K and the other in the 653–1038 K temperature ranges. The first step in Na-Mont has been ascribed to physisorbed and hydrating water, whereas the second is due to dehydroxylation of the silicate structure. Sometimes, this step occurs dissociated in two, hardly visible here but clearly shown in the corresponding DTG and, more so, in the ATD curve, denoting dehydroxylation of the silicate structure in two different environments, here Al and Mg, as a result of an important isomorphic substitution in the clay net with different bonding strengths between the Me and the surrounding oxygen (or hydroxyl) ions [18].

For every set of conditions, the steps in the thermal curves corresponding to the Zr-pillared clays, *i.e.* the losses in every thermal interval, show different intensities depending on the Zr content and the preparation method. For convenience, TG patterns have been

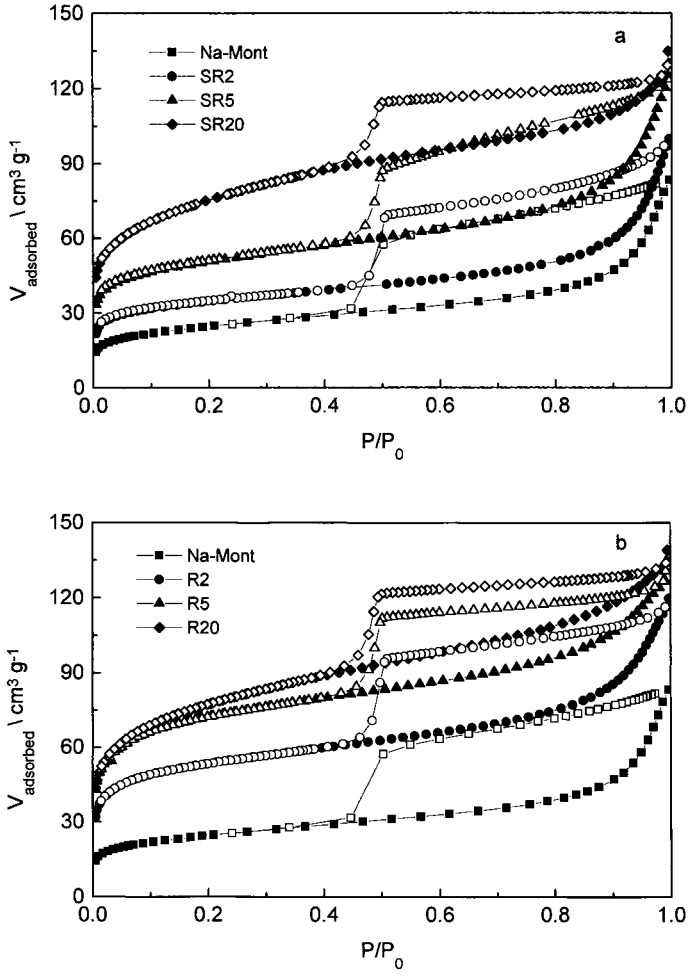

Fig. 2. N_2 adsorption-desorption isotherms: filled symbols, adsorption; open symbols, desorption: (a) SR series; and (b) R series.

separated into four temperature regions: 298(RT)–653, 653–873, 873–1038 and 1038–1273 K. In Table 2, the losses corresponding to every region of both, the parent clay and pillared samples after different thermal treatment are presented: UT is for ambient temperature; MT after 2 h treatment at 623 K and HT after 2 h treatment at 773 K. It must be stressed that all Zr samples experience percent weight losses higher than Na-Mont and higher than could be expected from the addition of the losses corresponding to both the components, Zr-tetramer and montmorillonite.

In the untreated samples (Fig. 3(a)), the first loss is different and roughly proportional to their Zr content, except in the sample 20R; it can be ascribed to the loss of physisorbed and interlamellar water from the cations present, Na^+ cations not totally exchanged and still remaining in the samples, and Zr polycations, but also, and more important, to an additional loss due to fixation of the hydroxy Zr species to the clay structure through condensation of the –OH groups and the corresponding water evolution.

The outline of the 653–1038 K interval, is clearly different from that in the parent clay, showing a nearly continuous decay instead of the step shown above; it results from a higher weight loss in the II region of the curve (653–873 K) followed by a smaller one in the III region (873–1038 K) with respect to Na-Mont. How-

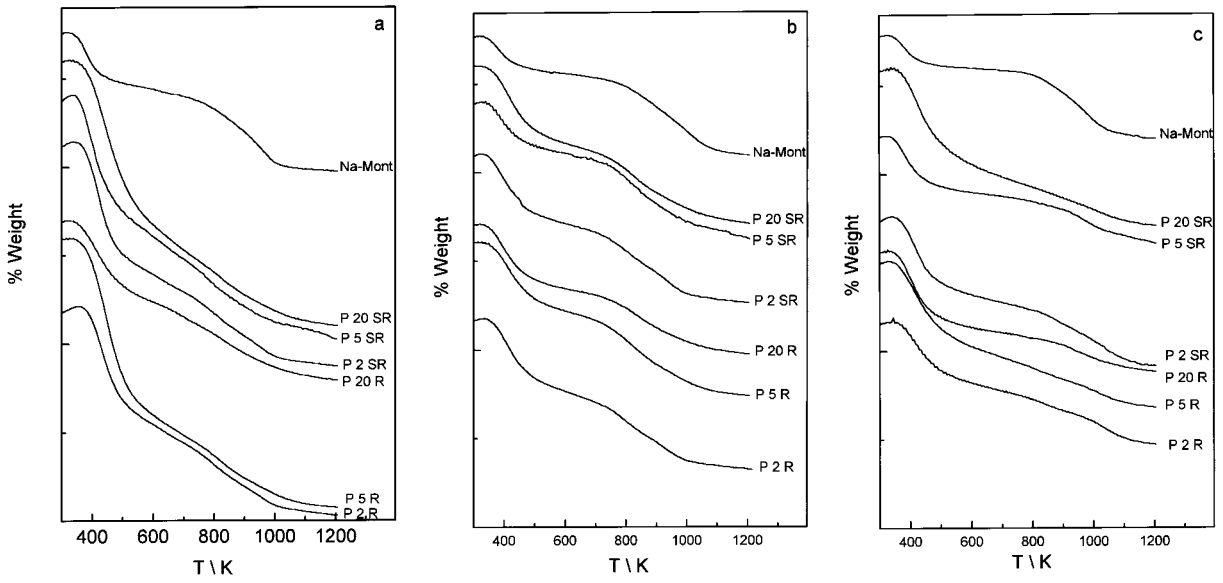

Fig. 3. TGA curves of Na-Mont and pillared materials after various thermal treatments: (a) untreated samples; (b) after 2 h treatment at 623 K; and (c) after 2 h treatment at 773 K.

Table 2
Percent losses of the samples treated at various temperatures

Sample	RT–653 K			653–873 K			873–1038 K			1038–1273 K			Total		
	UT [a]	MT [b]	HT [c]	UT [a]	MT [b]	HT [c]	UT [a]	MT [b]	HT [c]	UT [a]	MT [b]	HT [c]	UT [a]	MT [b]	HT [c]
Na-M	3.38	2.2	1.88	1.80	1.43	0.99	2.36	2.3	2.36	0.42	0.33	0.32	7.96	6.26	5.55
P2SR	7.78	4.12	4.44	2.63	2.20	1.16	1.62	1.65	1.64	0.42	0.37	1.09	12.45	8.34	8.33
P5SR	8.32	4.31	5.03	2.98	2.27	1.38	1.31	1.46	1.07	0.86	0.37	0.69	13.47	8.41	8.17
P20SR	10.05	4.63	5.68	2.90	2.25	1.33	1.47	1.44	1.10	0.72	0.62	0.70	15.14	8.94	8.81
P2R	6.87	2.93	3.59	2.65	2.35	1.17	1.55	1.51	1.17	0.42	0.45	0.92	11.49	7.84	6.85
P5R	10.56	4.09	3.28	2.66	2.46	0.74	1.47	1.55	1.36	0.57	0.53	0.81	15.16	8.63	6.19
P20R	4.94	3.8	4.42	2.26	1.75	0.66	1.29	1.26	1.11	0.61	0.49	0.57	9.07	7.30	6.76

[a] Untreated samples.
[b] Samples after 2 h, 623 K thermal treatment.
[c] Samples after 2 h, 773 K thermal treatment.

ever, the total loss in this interval is nearly equal in all samples, natural and pillared, except 20R, changing only the sequence of the losses.

The foregoing denotes, on the one hand, that the fixation of the polycations has been completed below 653 K and, on the other, that the Zr species are located near an Mg environment, as should be expected from the position of the exchangeable cations in the clay, straining locally the structure of the net, loosening the structural bonds there and prompting, at last, dehydroxylation and water evolution at a lower temperature than on the parent material. The effect is smaller in series R, which probably should be related to the position, mostly superficial, of Zr species on the delaminated clay. It must be emphasised that sample 20SR loses more, and 20R less, than the rest of the samples.

No additional loss with respect to Na-Mont is visible in the IV region of the TG curve (>1038 K), corresponding to the samples with the smaller Zr content, but there is some loss in the rest, roughly proportional to their Zr content. Following the works

of Occelli [19,20], Zr pillars begin to decompose above 813 K, but, here, the effect is only visible above 1038 K. Besides, the losses are slightly smaller in the R series, which also points to the presence of different Zr pillaring species in the samples. Sham [21] reported that, depending on the polymerization conditions, different types of ZrO_2 can be produced, giving rise to two-dimensional ordered structures with terminal –OH, or to three-dimensional ordered structures, the –OH bridging the various Zr elements. Also, following Burch and Warburton [4], under refluxing conditions larger cations than the tetramer should be expected. If so, water evolution will be different and smaller in the last case, because the number of –OH present by Zr unity is smaller. However, it is not the only effect here, because it does not appear in sample 2R and it is more important in 5R than in 20R samples, both of them synthesized under the same drastic conditions. In our opinion, the losses result from a combination of two effects: the incorporated Zr species and the presence of a partially destroyed clay resulting from leaching of the octahedral layer in the synthesizing step. Both effects are related to the pH of the starting Zr solution and are specially visible on sample 20R, which has been synthesized at 1.96 pH, the lowest of them all.

From the foregoing, it can be inferred that a pH <2.75 (as maximum) is harmful for the clay structure, and probably for the Zr tetrameric formation also, giving rise to higher polymers and, finally, to $Zr(OH)_x$ [22]; both effects justifying the smaller losses detected.

After the 623 K thermal treatment (Fig. 3(b)), no substantial changes in the thermal curves with respect to the untreated samples are observed. Total losses are much lower here, but still higher than those corresponding to the parent clay after the same treatment; again, the 653–873 K step is specially affected in all the samples, the effect increasing with the content of Zr and the severity of the preparation conditions. From the table, it is apparent that the materials have lost structural water during the thermal treatment, more in the SR than in the R series, which confirms the different behaviours of the Zr species and/or the corresponding interaction with the net as a result of the position of the cation in the clay, which is superficial in the delaminated and interlamellar in the pillared samples. As above, sample 20R behaves differently from the rest, experiencing a much lower loss, and thus confirming the above statements.

The 773 K treatment seems to have caused an important dehydroxylation of the materials because the total losses in the corresponding thermal curve (Fig. 3(c)) are much lower. But, more important, it seems to have produced an important weakening of the clay net, since the losses in the last step of the curve are much higher than after the preceding treatment. As it has been reported [23], dehydroxylation of hydroxycations releases protons; the higher the temperature the greater is the release of protons, which affects the clay structure, mainly the octahedral layer, prompting water formation and evolution. The structure of the clay must have been partially destroyed during the thermal treatment, diminishing the possibility of an additional dehydroxylation in the 623–1038 K interval. In contrast, the retained protons act above 1038 K, resulting in a more complete dehydroxylation of the clay to the corresponding oxides.

4.2. Differential thermal analysis

Thermogravimetric analysis have been completed by DTA. Fig. 4(a) is for Na-Mont and Fig. 4(b) and (c) are, respectively, for the pillared materials at RT and after calcination at 623 K.

The DTA plot corresponding to Na-Mont (Fig. 4(a)) shows an endothermic peak at low temperatures, below 573 K, which is not well resolved into two peaks, with maxima at around 373 and 453 K. It is generally interpreted as being caused by the loss of weakly bonded, physisorbed water adsorbed on the external surface of the clay, and of interlamellar water coordinated to the exchangeable cations, in this case Na^+. A shoulder visible at 610 K arises because of the interlamellar water loss, not easily evolved by diffusion from the sample or, most probably, it may be an artifact resulting from a combination of the two adjacent peaks. The next two peaks appear from dehydroxylation of the clay octahedral layer in different environments, at 752 K from Al substituting Mg (or Fe) and at 916 K from Al [18]. Both these endothermic peaks correspond to the losses detected by TG in the same interval. Finally, an endothermic peak at around 1106 K is due to the final dehydroxylation and crystalline net destruction. According to Grim [24], this type of materials should present an S-shaped endo- exothermic peaks the first part corresponding to the loss of structural water without

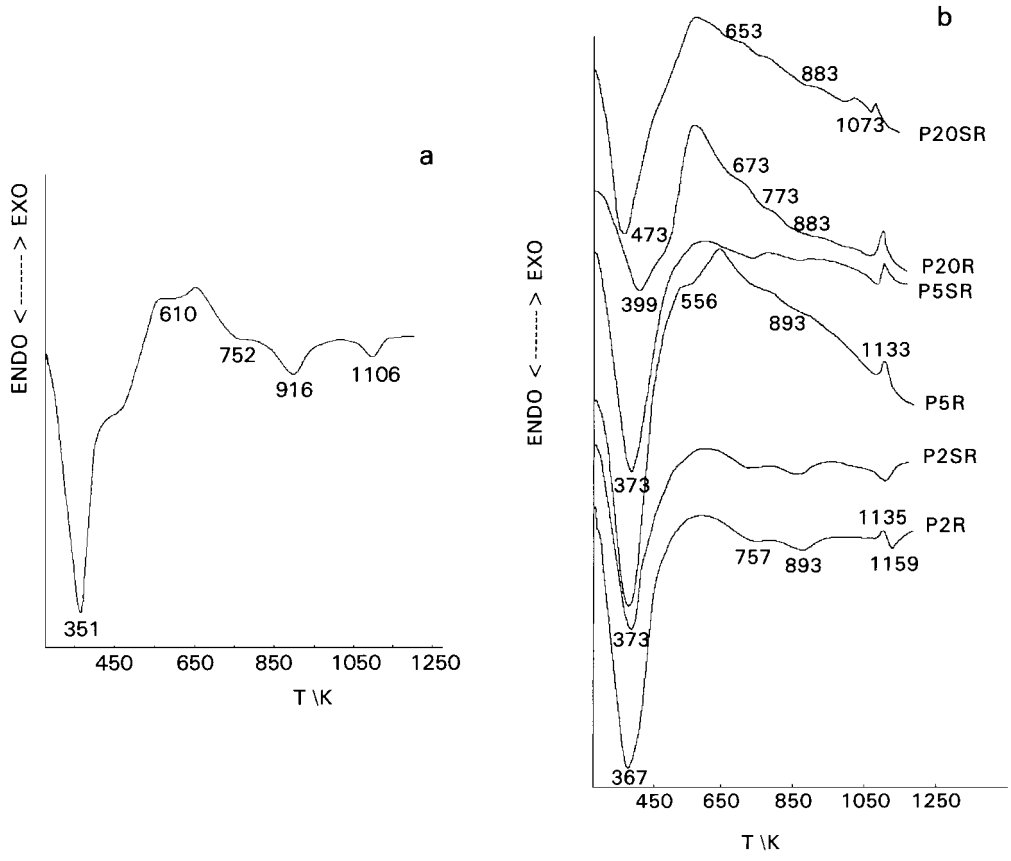

Fig. 4. Differential thermal analysis (DTA) of Na-Mont and pillared samples: (a) Na-Mont, untreated; (b) pillared samples, untreated.

destroying the crystalline net which persists up to higher temperatures and, the second part (exothermic peak) to changes constituting a new structure of α-quartz or mullite, depending on the nature of the montmorillonite involved. This second peak is not visible here, probably because the high content of interchanged Na impedes the final transformation of the clay [18].

The DTA curves for the untreated pillared clays (Fig. 4(b)) do not depart so much from the parent material, however, some differences appear: the larger the content of Zr and the harder the preparation conditions of the cation, the greater the difference. Thus, samples P2 and P5SR preserve a plot similar to the original Na-clay, only differing from it in the peak intensities, especially in the initial endothermic peak which gets a certain asymmetry. A general feature of the curves is the disappearance of the endothermic peak at around 453 K, which in the Na-Mont corresponds to the Na-hydrating water. In the first terms of the series 2SR and 2R, only a certain asymmetry appears, probably due to a gradual and continuous loss of water from hydrated Na still remaining in the sample after the incomplete exchange experienced and the Zr hydroxycations incorporated. In the remaining samples, a shoulder is visible, arising from the dehydroxylation of Zr species, and subsequent interaction with the clay.

One additional characteristic of the curve is the loss of definition of the peaks at around 752 and 916 K, visible in case of Na-Mont, specially in the last terms of the series. These peaks in the parent clay were attributed to dehydroxylation from different environments, and related to the position of the exchangeable cations in the clay. Here, both peaks grow smaller, more the peak at 916 K which

show to a lower temperature, confirming the TG results.

A new peak at around 773 K appears in the samples with the larger Zr content, 20RS and 20R. This peak probably can be related to the exothermic one detected by Sham [21] in a Zr/SiO_2–Al_2O_3 sample synthesized at low pH (<3) when the concentration of zirconia was >6.7%; there, the peak was related to the change from an amorphous to the tetragonal form of ZrO_2. Its appearance here, probably denotes the presence of amorphous ZrO_2 not linked to the clay net.

The last point to be emphasized is the appearance of a very broad exothermic peak starting at around 523 K and ending near 893 K, superposed on the remaining peaks in the samples synthesized at the lower pHs (5R, 20SR and 20R). Burch and Warburton [4] ascribed that broad exotherm to the chemical interaction between the pillars and the clay layers to form a stable bond. However, the exotherm does not occur in sample 5SR, with the same Zr content than 5R but obtained under less drastic conditions; besides, the fixation of the pillars to the clay net occurs below 653 K, as shown by TGA. In our opinion, the effect is related to the continuous change of the amorphous alumina or silica resulting from leaching of the octahedral sheet under the low pH in the pillaring step and present in the samples.

Above 1000 K, all Zr-pillared samples, except 2SR and 2R, apart from the parent material. Present the S-shaped endo-exothermic peaks that should be expected from the type of clay involved; since interchange was completed only above 5% Zr, the stabilizing effect of Na, visible on Na-Mont, only acts on samples 2R and 2SR. The final exothermic peak is similar in all the remaining samples, denoting thereby that the ZrO_2 present does not interfere with the rearrangement of the clay structure.

The DTA curves of the samples treated at 623 K (Fig. 5) are quite similar to the previous ones, the only difference being, once again, the extension of the endothermic peak which is related to physisorbed water evolution in a non-equilibrated environment and also to the presence of Zr species which have not yet dehydroxylated under the applied thermal treatment. More significant is the disappearance of the 523–893 K exotherm in samples 5R and 20SR and the change in 20R from an exo- to an endopeak, which probably can be related to the clay degradation

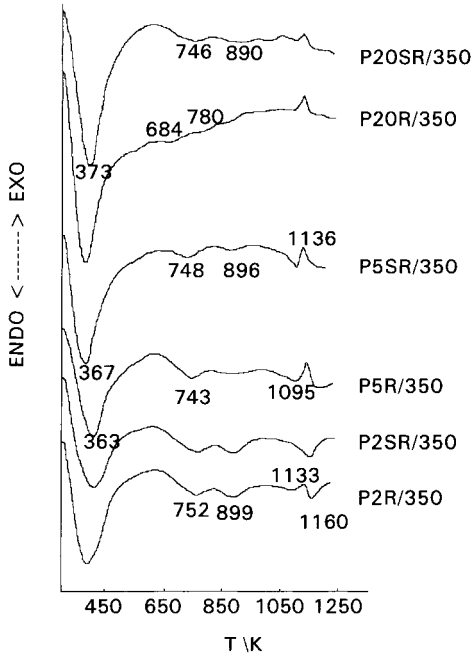

Fig. 5. DTA of PZr after 2 h treatment at 623 K.

because of the protons released during the thermal treatment and still present in the net. Also, the appearance of the 684 K peak, probably a shift of that at 748 K, confirms this effect, whereas the persistence of the peak around 7730 K in the more Zr charged samples shows that the change from amorphous to tetragonal ZrO_2 is not affected by the protons released. Finally, the characteristics of the peaks above 1073 K are quite similar to that of untreated samples, thus confirming the previous statements.

4.3. FTIR spectra

The changes in the clay structure caused by Zr incorporation, must be visible by FTIR. In Fig. 6(a) and (b), the FTIR spectra corresponding to all samples after calcining at 623 K are presented. The spectrum corresponding to Na-Mont is also included for comparison.

Observing the IR spectrum corresponding to the parent material, Na-Mont, two peaks at 3626 and 3448 cm^{-1} are noticed in the OH stretching region. The pattern is typical of water adsorbed in dioctahedral 2 : 1 layer silicates: a fairly narrow band at ~3620 cm^{-1}, ascribed [25] to the stretching vibration

of –OH in Al_2OH hydroxyl absorption of randomly oriented samples, and a broad maximum near 3400 cm^{-1} corresponding to hydroxyl groups involved in water–water hydrogen bonds. This stretching vibration has the corresponding bending mode at ~1630 cm^{-1}. The peak at 1039 cm^{-1} corresponds to the perpendicular Si–O–Si antisymmetric vibration when substitution of Al for Si is low; Al_2OH libration lies in the 915–950 cm^{-1} range, and Mg substitution for Al in MgAlOH, at 844 cm^{-1}. A peak at 795 cm^{-1}, together with those at 520 and 460 cm^{-1}, can be ascribed to Si–O bending vibration. Unfortunately,

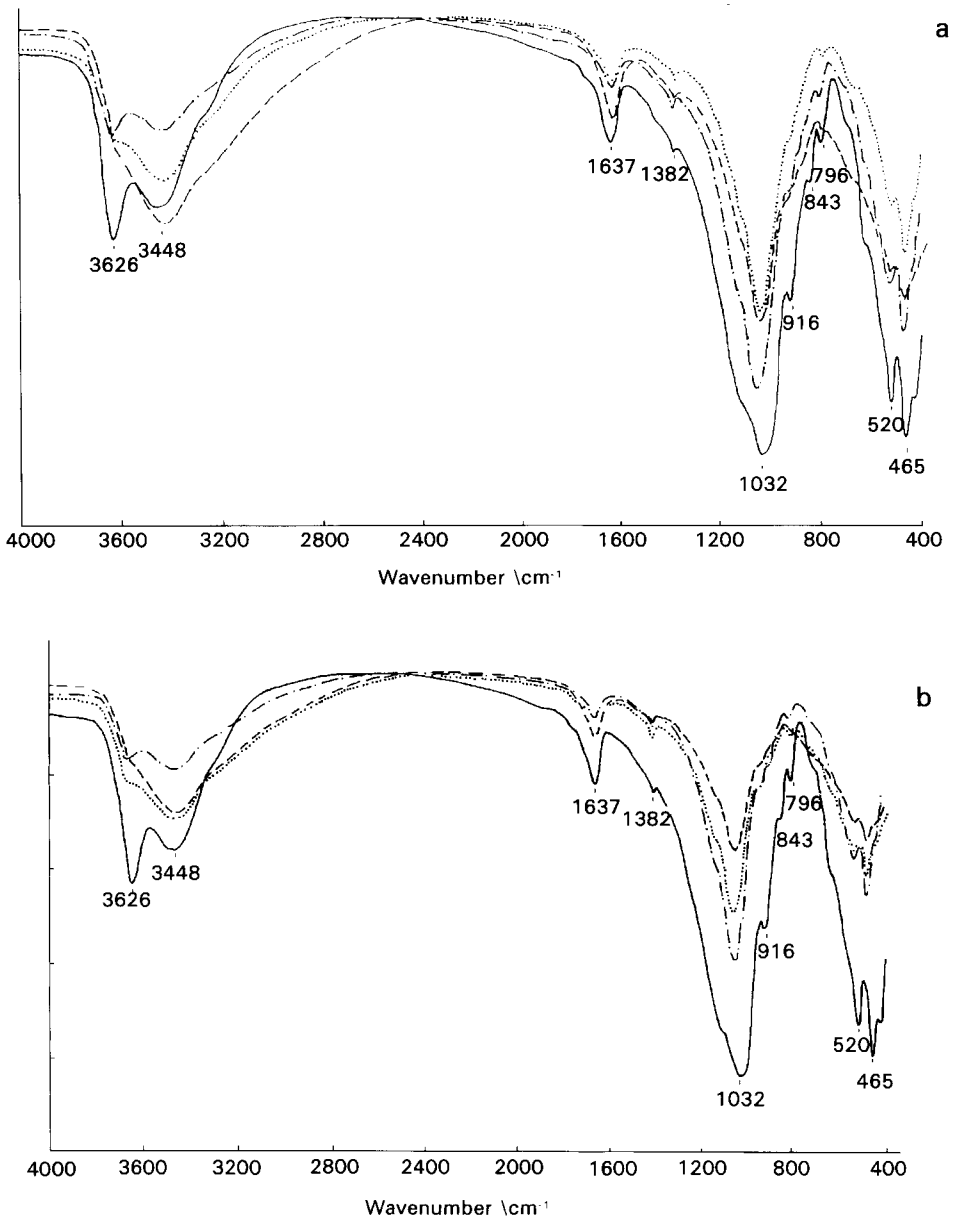

Fig. 6. FTIR spectra of the samples after 350°C calcination: (———), Na-Mont; (– · –), P2; (. . .), P5; (- - -), P20. (a) Series SR; and (b) series R.

we cannot see the lower frequency (<400 cm^{-1}) region and thus the effect of the interlayered cations (<100 cm^{-1}) cannot be identified.

Comparing the spectra corresponding to P-Zr samples with the previous one, an increase of the back-absorption is primarily observed due to the hydrated species occurring after the synthesis processes. Besides, a decrease of the 3620 cm^{-1} peak together with the appearance of a width shoulder below 3300 cm^{-1} is visible, denoting the change in the clay structure provoked by the process. All peaks in the 1032–800 cm^{-1} range progressively decrease, and more so in the R series, with the Zr content. In contrast, a broad, poorly defined shoulder develops in the 550–750 cm^{-1} region, especially in the more treated samples. No noticeable difference has been detected in the bands at 520 and 465 cm^{-1} after pillaring.

In our opinion, all those changes must be related to, firstly, the incorporation of the Zr polycation to the hydroxylayer shown by the disappearance of Al_2OH stretching vibration (3626 cm^{-1}) and Al_2OH (916 cm^{-1}) and AlMgOH (843 cm^{-1}) libration bands and, secondly, the presence of small strongly polarizing cations such as Al^{3+} arising from cleavage of the octahedral layer in the pillaring step shown in the 3300 cm^{-1} shoulder. It is well known [25] that water molecules coordinate to those cations forming stronger hydrogen bonds to water in outer spheres of coordination, thus increasing the absorption below 3300 cm^{-1}. Finally, the decrease in the number of layered Si–O–Si bonds (1032 cm^{-1} peak) to form silica strongly coupled with vibrations of the octahedral cations partially liberated from the net after the protonic attack of the clay in the pillaring and further calcining steps (broad bands in the 750–550 cm^{-1} range).

Under increasing temperatures, a decrease in the back-absorption and in the peaks intensity, more visible at low frequencies (<1050 cm^{-1}), is observed. Fig. 7 depicts the changes experienced by sample P5R taken as an example. A similar behaviour has been detected by Sun [26] and Comelli et al. [27] in Al-pillared clays and by Calvet [28], and Tennakoon [29,30] on calcining Li^+-, NH_4^+- and Al^{3+} exchanged clays. Following those authors, later confirmed by Fripiat on Al-PILC [23], the protons liberated on grafting the polyoxycations to the clay, diffuse under heating inwards the clay structure and promote water evolution from combination with the –OH of the net [31]. This self-destructive protonic attack, which reveals the dehydroxylation within the pillared clay, occurs in the 573–873 K interval, as in our experiment. Yariv and Heller-Kallai [32] relate the decrease in the intensity of the 919 cm^{-1} peak, to the diffusion of the protons released from the pillars into the octahedral sheet, and subsequent water formation with the structural –OH from Al_2OH. Schutz [33] also detected the progressive reduction in intensity of the 3450 cm^{-1} peak, which he also ascribed to the protons released from the pillars which may either enter the octahedral sheet combining with structural hydroxyl groups to form water, or react with tetrahedral Si–O–Al bonds (the weaker bonds) to give Si–OH and Al–OH. In our opinion, and since we have observed the decrease in both zones 3400 cm^{-1} and 916–842 cm^{-1}, we accept the former interpretation.

5. Conclusions

The results presented here show that parameters, such as the concentration of the Zr solution, pH, temperature and time of contact with the clay, can affect the hydrolytic chemistry of the pillaring agent and, consequently, the fundamental properties of the final product. The pH of the starting Zr solution is, in particular, of utmost importance in getting the proper Zr species and pillared materials. Under reflux conditions and at high zirconyl-chloride concentrations, cations larger than the tetramer are formed; moreover, the pH of the resulting pillaring solution affects the stability of the clay. Zr/clay ratios around 2, either refluxed or not, result in a thermally unstable material, due to the scarce presence of the pillars in the clay interlayer, and it collapses at temperatures higher than 623 K. In contrast, relations around 20 meq/g clay and, when reflux is used in the preparation of the cations result in barely pillaring but delamination of the parent clay; besides, under such conditions, zirconia or Zr-polyhydroxycations deposit on the lamellae as amorphous zirconia which, under thermal treatment, changes to tetrahedral ZrO_2. We found that only the samples prepared from unrefluxed Zr solutions and with Zr/clay ratios between 2 and 20 meq/g result in stable pillars.

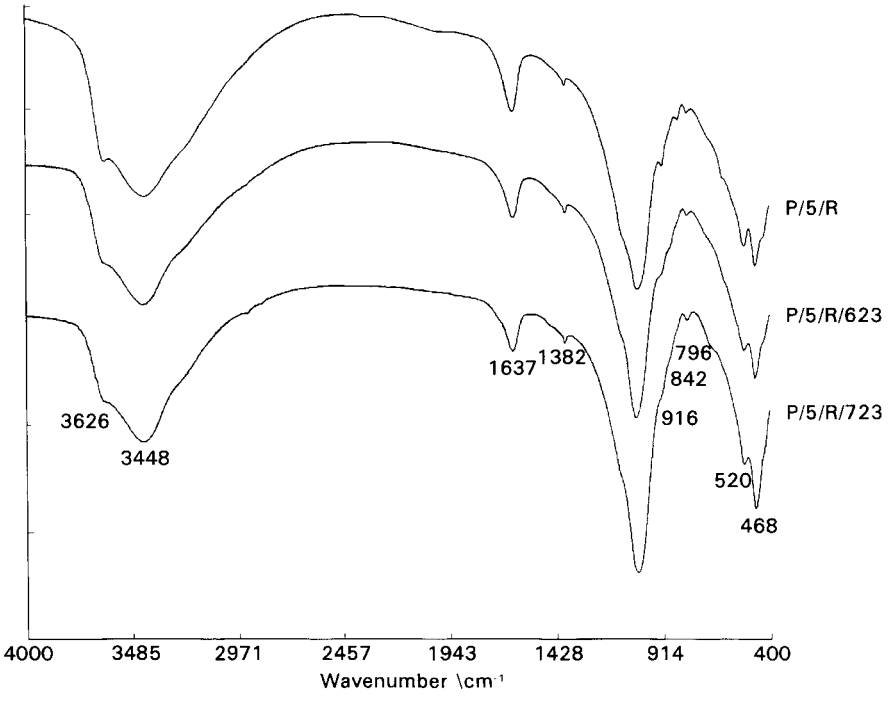

Fig. 7. FTIR spectra of sample P5R after various temperature treatments.

In our opinion, the Yamanaka–Brindley method is perfectly suited for preparing Zr pillared samples, and the determining factor of synthesis is the pH of the Zr pillaring solution more than the Zr species formed. A limit for the stability of the parent clay used in this work is ~2.7 pH. Below this value, the parent clay delaminates and hardly any pillaring results from the synthesis.

As a consequence of the various Zr species present, the dehydroxylation of the Zr-PILC precursors follows different patterns. Normally, it starts at around 523 K and can be followed by the shape of the DTA curve which can be used as an indicator of the appropriateness of the pillaring process.

Thermal analysis, together with IR spectroscopy, has shown that excess of protons, whatever their source, are responsible for the thermal unstability of pillared clay.

Acknowledgements

The authors are truly indebted to the CICYT for the material support to this work under Project MAT95-0143-C02-01. M.R. Sun Kou acknowledges the ICI for the scholarship who enabled her to get her Ph.D degree. Our thanks to Minas de El Gador for the kind donation of the smectite sample.

References

[1] I.V. Mitchell, Pillared Layered Structures, Current Trends and Applications, Elsevier Applied Sciences, London, 1990.
[2] F. Figueras, Catal. Rev. Sci. Eng. 30 (1988) 457.
[3] S. Yamanaka, G.W. Brindley, Clays Clay Miner. 27 (1979) 119.
[4] R. Burch, C.I. Warburton, J. Catal. 97 (1986) 503.
[5] G.J.J. Bartley, R. Burch, Appl. Catal. 19 (1985) 175.
[6] A. Clearfield, P.A. Vaughan, Acta Crystallogr. 9 (1956) 555.
[7] T. Lopez, M. Asomoza, R. Gomez, Thermochim. Acta 223 (1993) 233.
[8] M.L. Occelli, in L.G. Schutz, H. van Olphen, F.A. Mumpton (Eds.), Proceedings Intern. Clay Conf., Denver 1985. The Clay Minerals Society, Bloomington, Indiana, 1987.
[9] M.L. Occelli, D.H. Finseth, J. Catal. 99 (1986) 316.
[10] T.M. El-Akkad, N.S. Felex, N.M. Guindy, S.R. El-Massry, S. Nashed, Termochim. Acta 59 (1982) 9.
[11] V.C. Farmer, J.D. Russell, Spectrochim. Acta 20 (1964) 1149.
[12] V.C. Farmer, J.D. Russell, Clays Clay Miner. 15 (1967) 121.

[13] C.S. Ross, S.B. Hendricks, Minerals of the montmorillonite group, Prof. pap. U.S. Geol. Survey No. 205-B, Washingtonm, 1945, p. 23.
[14] M.M. Dubinin, L.V. Raduskevitcht, Proc. Acad. Sci. USSR 55 (1947) 331.
[15] M.L. Occelli, Catal. Today 2 (1988) 339–356.
[16] S. Mendioroz, J.A. Pajares, I. Benito, C. Pesquera, F. Gonzalez, C. Blanco, Langmuir 3 (1987) 671–676.
[17] K.A. Carrado, A. Kostapapas, S.L. Suib, Solid State Ionics 22 (1986) 117–125.
[18] P. de Souza Santos, in Edgard Blücher Ltda (Ed.), Tecnologia de argilas, Vol. 1, Sao Paulo, 1975, pp. 277–302.
[19] M.L. Occelli, J. Mol. Catal. 35 (1986) 377.
[20] M.L. Occelli, R.M. Tindwa, Clays Clay Miner. 31 (1983) 22.
[21] E.L. Sham, S. Bruque, J.J. Rodriguez, Actas del XIII Simposium Iberoamericano de Catálisis, Segovia, 1992.
[22] F. Baes, R.E. Mesmer, in R.E. Krieger (Ed.), The Hydrolysis of Cations, Publishing Company, Florida, 1986.
[23] J.J. Fripiat, Pillared Clays, Catal. Today 2(2–3) (1988) 281.
[24] R.E. Grim, R.A. Rowland, Amer. Min. 27 (1942) 746.
[25] V.C. Farmer, in V.C. Farmer (Ed.), The Infrared Spectra of Minerals, Mineralogical Society, 1974.
[26] M.R. Sun Kou, Ph.D. Thesis, Complutense University of Madrid, Spain, 1994.
[27] R.A. Comelli, C.R. Vera, J.M. Parera, Latin American Appl. Res. 24 (1994) 227.
[28] R. Calvet, R. Prost, Clays Clay Miner. 19 (1971) 175.
[29] D.T.B. Tennakoon, T.A. Carpenter, W. Jones, J.M. Thomas, S. Ramdas, J. Chem. Soc. Faraday Trans. 82 (1986) 545.
[30] D.T.B. Tennakoon, W. Jones, J.M. Thomas, J.H. Ballantine, L. Purnell, Solid State Ionics 24 (1987) 205.
[31] D. Tichit, F. Fajula, F. Figueras, B. Ducourant, G. Mascherpa, C. Gurguen, J. Bosquet, Clays Clay Miner. 36 (1988) 369.
[32] S. Yariv, L. Heller-Kallai, Clays Clay Miner. 21 (1973) 199.
[33] A. Schutz, W.E.E. Stone, G. Poncelet, J.J. Fripiat, Clays Clay Miner. 35 (1987) 251.